General Explicit Mathematical Solution for the Voltammetry of Nonunity Stoichiometry Electrode Reactions: Diagnosis criteria in Cyclic Voltammetry

José María Gómez-Gil, Eduardo Laborda*, Angela Molina*

Departamento de Química Física, Facultad de Química, Regional Campus of International Excellence "Campus Mare Nostrum", Universidad de Murcia, 30100 Murcia, Spain

* Corresponding authors:

Tel: +34 868 88 7524

Fax: +34 868 88 4148

Email: amolina@um.es; elaborda@um.es

ABSTRACT

Electrochemical reactions can effectively follow nonunity stoichiometries as can be found in the electrochemistry of halides, hydrogen and metal complexes. The voltammetric response of these systems shows peculiar deviations with respect to the well-described features of the 1:1 stoichiometry. With the aim of specifying such differences, a rigorous and manageable analytical theory is deduced for the complete characterization of reversible electrode processes with complex stoichiometry in cyclic voltammetry (CV) at macroelectrodes. Particularly, the main features of the CV of 2:1, 1:2, 3:1 and 1:3 processes (that is, the peak currents and potentials and the influence of the scan rate and of the species concentration and diffusion coefficients) are given and compared with the 1:1 case in order to propose unambiguous diagnostic criteria of the stoichiometry of the electrode reaction. Also, expressions for the concentration profiles and surface concentrations of the redox species are given.

INTRODUCTION

The global reaction scheme of key electron transfer processes show non-unity stoichiometry such as it is the case of the electro-oxidation of the hydride ion in molten salts[1]:

$$2H^- - 2e^- \rightleftarrows H_2$$

the electro-oxidation of halide anions (X^-)[2–5]:

$$3X^- \rightleftarrows X_3^- + 2e^-$$

and the electro-oxidation of mercury in complexing media[6–9]:

$$\left(Hg + \right) jL \rightleftarrows HgL_j + 2e^- \quad (j=1\text{-}4)$$

The above processes follow multistep mechanisms where several electron transfers are coupled to heterogeneous or homogeneous physicochemical processes such as the adsorption-desorption [10] or chemical reaction of intermediates. When such different steps are fast and reversible, the overall response of the system will approach, *apparently*, that of the following *a:b* E scheme:

$$aO + ne^- \rightleftarrows bR \qquad (I)$$

that is, it will be perceived phenomenologically as the simultaneous transfer of *n* electrons to *a* molecules of reactant yielding *b* molecules of product. This has been reported, for example, for the hydrogen-hydride couple at Cu in LiCl-CsCl melts [1] and the Hg(II) thiocyanato complexes-mercury pair [9]. Also, Scheme (I) with *a*=2, *n*=2 and *b*=1 has been proposed in previous literature for the proton-hydrogen redox couple at Pt electrodes and nanoparticles [11–13].

In spite of the seeming simplicity of the theoretical treatment of these processes, a general analytical explicit resolution of the boundary value problem (bvp) corresponding to Scheme (I) in voltammetry has not been possible in spite of the efforts made over decades. Thus, analytical solutions for the current-potential response of complex stoichiometries are only available under steady state conditions[3,14] and in single pulse polarography[15], including the expressions for the half-wave potential. To the best of our knowledge, no analytical explicit solutions have been deduced for the current-

potential response, the concentration profiles (essential in spectroelectrochemistry) and the surface concentrations in multipulse techniques under transient conditions.

In order to fill the gap above-mentioned, a general analytical treatment of reversible electron transfers of complex stoichiometry at macroelectrodes is developed in this work, finding the general mathematical form of the concentrations profiles and the relationship between the surface concentrations of the redox species for any stoichiometry, any voltammetric technique and any diffusion coefficients. Among other aspects, the present theoretical study demonstrates rigorously the relationship between the surface concentrations of the redox species, as well of their time independence under linear diffusion and Nernstian conditions, so that the superposition principle is applicable. This also proves that the bvp for any *a:b* stoichiometry is mathematically identical to that of a 1:1 process, the only additional difficulty being the calculation of the values of the surface concentrations by simply solving a system of algebraic equations. Moreover, the theory presented can be used as a first approach to this kind of electron transfer processes, enabling the *a priori* analysis of the system's chief variables and particular behaviours as well as serving as a reference for the validation of more complex models.

Exact explicit solutions are deduced for the concentration profiles, the surface concentrations and the current-potential response of the 2:1, 1:2, 3:1 and 1:3 mechanisms considering that both the oxidized and reduced species are initially present in solution. The particular features of the cyclic voltammetry of these complex stoichiometry mechanisms, as compared with the 1:1 case, are analysed, discussing their characteristic features and behaviours that serve as diagnosis criteria and guidelines for quantitative analyses.

THEORY

Let us consider the process depicted in Scheme (I) behaving reversibly and implying the apparently simultaneous transfer of *n* electrons to *a* molecules of reactant O (Scheme I) upon the application of a constant potential pulse (E), it can be demonstrated (see Supporting Information) that the diffusion problem can be reduced to a single variable problem so that the surface concentrations are constant and the concentration profiles of the redox species ($c_O(x,t)$, $i \equiv O, R$) have the following mathematical form whatever the *a*:b stoichiometry[16]:

$$c_O(x,t) = c_O^* + \left(c_O^s - c_O^*\right) \operatorname{erfc}\left(\frac{x}{2\sqrt{D_O t}}\right)$$
$$c_R(x,t) = c_R^* + \left(c_R^s - c_R^*\right) \operatorname{erfc}\left(\frac{x}{2\sqrt{D_R t}}\right) \quad (1)$$

where *x* refers to the distance to the electrode surface, *t* to the time of the perturbation, $c_i^* \left(i \equiv O, R\right)$ to the bulk concentrations of the redox species, c_i^s to their surface concentration and D_i to their diffusion coefficient. Eqs. (1) imply that the linear diffusion layer is given by the same expression ($\sqrt{\pi D t}$) for any values of the stoichiometric coefficients.

By inserting Eqs. (1) into the mass conservation condition (see Eq. (SI.3) in the Supporting Information), the following general relationship is immediately deduced for the surface concentrations:

$$b\sqrt{D_O}c_O^s + a\sqrt{D_R}c_R^s = b\sqrt{D_O}c_O^* + a\sqrt{D_R}c_R^* \quad (2)$$

Note that this has been derived here rigorously, verifying its previous use based on "intuition" under transient conditions [17].

When the redox species show equal diffusion coefficients ($D_O = D_R$), from Eqs. (1) and (2) it is readily proven that the above relationship (2) holds at any point in solution (and moment of the experiment), that is:

$$bc_O(x,t) + ac_R(x,t) = bc_O^* + ac_R^* \quad (\forall\, x, t) \quad (3)$$

Also, from Eqs. (1) the current response is deduced to have the following form:

$$\frac{\mathrm{I}}{nFA} = \frac{D_{\mathrm{O}}}{a}\left(\frac{\partial c_{\mathrm{O}}}{\partial \mathrm{x}}\right)_{\mathrm{x}=0} = \frac{D_{\mathrm{O}}}{a}\frac{\left(c_{\mathrm{O}}^{*} - \mathrm{c}_{\mathrm{O}}^{\mathrm{s}}\right)}{\sqrt{\pi D_{\mathrm{O}} t}} \tag{4}$$

where *n* is the number of electrons and *A* the electrode area. From Eq. (4), a general expression for the half-wave potential ($E_{1/2}$) is obtained [9,11,14]:

$$E_{1/2} = E^{0'} - \frac{RT}{nF} b \ln(\gamma) + \frac{RT}{nF} b \ln\left(\frac{a}{b}\right) + \frac{RT}{nF}(a-b)\ln\left(\frac{\mathrm{c}_{\mathrm{O}}^{*} + \frac{a}{b}\frac{\mathrm{c}_{\mathrm{R}}^{*}}{\gamma}}{2}\right) \tag{5}$$

where $E^{0'}$ is the formal potential of the redox couple O/R,

$$\gamma = \sqrt{\frac{D_{\mathrm{O}}}{D_{\mathrm{R}}}} \tag{6}$$

and $\mathrm{c}_{\mathrm{O}}^{*}$ and $\mathrm{c}_{\mathrm{R}}^{*}$ are on the molar scale. Note that the half-wave potential under linear diffusion conditions shows a logarithmic dependence with the *square root* of the ratio between the diffusion coefficients, while under steady state conditions such dependence is with the ratio $D_{\mathrm{O}} / D_{\mathrm{R}}$.

The 2:1, 3:1, 1:2 and 1:3 stoichiometries

Manageable explicit expressions for the surface concentrations and for the current-potential response can be obtained for the 2:1 and 3:1 stoichiometries. Thus, by combining the surface Nernstian condition (see Eq. (SI.4) in the Supporting Information) with Eq. (2), the following expressions for $\mathrm{c}_{\mathrm{O}}^{\mathrm{s}}$ and $\mathrm{c}_{\mathrm{R}}^{\mathrm{s}}$ are deduced:

$$\left.\begin{aligned} \mathrm{c}_{\mathrm{O}}^{\mathrm{s}} &= \left(\mathrm{c}_{\mathrm{O}}^{*} + \frac{2}{\gamma}\mathrm{c}_{\mathrm{R}}^{*}\right)\left(\frac{\sqrt{e^{2\eta} + 8e^{\eta}} - e^{\eta}}{4}\right) \\ \mathrm{c}_{\mathrm{R}}^{\mathrm{s}} &= \frac{\gamma}{2}\mathrm{c}_{\mathrm{O}}^{*} + \mathrm{c}_{\mathrm{R}}^{*} - \frac{\gamma}{2}\mathrm{c}_{\mathrm{O}}^{\mathrm{s}} \end{aligned}\right\} \ (2{:}1 \text{ stoichiometry}) \tag{7}$$

$$\left.\begin{aligned} c_O^s &= -\left(c_O^* + \frac{3}{\gamma}c_R^*\right)\sqrt{\frac{e^\eta}{3}}\sinh\left(\frac{1}{3}\operatorname{asinh}\left(-3\sqrt{\frac{3}{e^\eta}}\right)\right) \\ c_R^s &= \frac{\gamma}{3}c_O^* + c_R^* - \frac{\gamma}{3}c_O^s \end{aligned}\right\} \quad \text{(3:1 stoichiometry)} \tag{8}$$

and:

$$\eta = \frac{nF}{RT}\left(E - E_{1/2}\right) \tag{9}$$

with concentrations being referred on the molar scale. Thus, c_O^s and c_R^s for a discrete potential-time perturbation, the surface concentration are constant within each pulse, being only dependent on the potential applied in each moment and not on the previous history of the experiment. Hence, as demonstrated in [18], the superposition principle is applicable, which has important implications as discussed in the Supporting Information. Once c_O^s is known, the expression for the current response is immediately obtained from Eq. (4):

$$\frac{I}{nFA} = \frac{1}{2}\sqrt{\frac{D_O}{\pi t}}\left\{c_O^* + \left(c_O^* + \frac{2}{\gamma}c_R^*\right)e^\eta\left(\frac{1-\sqrt{1+\frac{8}{e^\eta}}}{4}\right)\right\} \quad \text{(2:1 stoichiometry)} \tag{10}$$

$$\frac{I}{nFA} = \frac{1}{3}\sqrt{\frac{D_O}{\pi t}}\left\{c_O^* + \left(c_O^* + \frac{3}{\gamma}c_R^*\right)\sqrt{\frac{e^\eta}{3}}\sinh\left(\frac{1}{3}\operatorname{asinh}\left(-3\sqrt{\frac{3}{e^\eta}}\right)\right)\right\} \quad \text{(3:1 stoichiometry)} \tag{11}$$

Attending to that the 1:2 and 1:3 mechanisms are mirror image of the 2:1 and 3:1 schemes, respectively, all the above solutions can be readily extended to the 1:2 and 1:3 situations by replacing η , c_O^*, D_O , c_R^* and D_R with $-\eta$, c_R^*, D_R , c_O^* and D_O , respectively. Thus, after some manipulations, one obtains:

$$\left.\begin{aligned} c_O^s &= c_O^* + \frac{c_R^*}{2\gamma} + \left(c_O^* + \frac{c_R^*}{2\gamma}\right)\left(\frac{1-\sqrt{1+8e^\eta}}{4e^\eta}\right) \\ c_R^s &= 2\gamma c_O^* + c_R^* - 2\gamma c_O^s \end{aligned}\right\} \quad \text{(1:2 stoichiometry)} \tag{12}$$

$$\left.\begin{aligned} c_O^s &= \left(c_O^* + \frac{1}{3\gamma}c_R^*\right)\left[1 + \sqrt{\frac{1}{3e^\eta}}\sinh\left(\frac{1}{3}\operatorname{asinh}\left(-3\sqrt{3e^\eta}\right)\right)\right] \\ c_R^s &= 3\gamma c_O^* + c_R^* - 3\gamma c_O^s \end{aligned}\right\} \quad \text{(1:3 stoichiometry)} \tag{13}$$

and:

$$\frac{I}{nFA}=\sqrt{\frac{D_{\mathrm{O}}}{\pi t}}\left\{\left(\mathrm{c}_{\mathrm{O}}^{*}+\frac{\mathrm{c}_{\mathrm{R}}^{*}}{2\gamma}\right)\left(\frac{\sqrt{1+8e^{\eta}}-1}{4e^{\eta}}\right)-\frac{\mathrm{c}_{\mathrm{R}}^{*}}{2\gamma}\right\}\quad\left(1{:}2\text{ stoichiometry}\right)\tag{14}$$

$$\frac{I}{nFA}=\sqrt{\frac{D_{\mathrm{O}}}{\pi t}}\left\{\mathrm{c}_{\mathrm{O}}^{*}-\left(\mathrm{c}_{\mathrm{O}}^{*}+\frac{1}{3\gamma}\mathrm{c}_{\mathrm{R}}^{*}\right)\left[1+\sqrt{\frac{1}{3e^{\eta}}}\sinh\left(\frac{1}{3}\operatorname{asinh}\left(-3\sqrt{3e^{\eta}}\right)\right)\right]\right\}\quad\left(1{:}3\text{ stoichiometry}\right)\tag{15}$$

Multipulse techniques

As detailed in the Supporting Information, the superposition principle is applicable in this problem, which enables us to obtain the following general expressions for the concentration profiles upon the application of any sequence of arbitrary potential pulses E_1, E_2,… E_m…, E_p:

$$\begin{aligned}c_{\mathrm{O}}^{(\mathrm{p})}(x,t)&=c_{\mathrm{O}}^{*}+\left(\mathrm{c}_{\mathrm{O}}^{(1)\mathrm{s}}-c_{\mathrm{O}}^{*}\right)\operatorname{erfc}\left(\frac{\mathrm{x}}{2\sqrt{D_{\mathrm{O}}t_{1\mathrm{p}}}}\right)+\sum_{m=2}^{p}\left(\mathrm{c}_{\mathrm{O}}^{(\mathrm{m})\mathrm{s}}-\mathrm{c}_{\mathrm{O}}^{(\mathrm{m}\text{-}1)\mathrm{s}}\right)\operatorname{erfc}\left(\frac{\mathrm{x}}{2\sqrt{D_{\mathrm{O}}t_{\mathrm{mp}}}}\right)\\ c_{\mathrm{R}}^{(\mathrm{p})}(x,t)&=\left(\mathrm{c}_{\mathrm{R}}^{(1)\mathrm{s}}-c_{\mathrm{R}}^{*}\right)\operatorname{erfc}\left(\frac{\mathrm{x}}{2\sqrt{D_{\mathrm{R}}t_{1\mathrm{p}}}}\right)+\sum_{m=2}^{p}\left(\mathrm{c}_{\mathrm{R}}^{(\mathrm{m})\mathrm{s}}-\mathrm{c}_{\mathrm{R}}^{(\mathrm{m}\text{-}1)\mathrm{s}}\right)\operatorname{erfc}\left(\frac{\mathrm{x}}{2\sqrt{D_{\mathrm{R}}t_{\mathrm{mp}}}}\right)\end{aligned}\tag{16}$$

where:

$$\left.\begin{aligned}t_{\mathrm{mp}}&=\sum_{j=m}^{p-1}\tau_{\mathrm{j}}+t_{\mathrm{p}}\quad(\mathrm{m}=1,2\ldots\mathrm{p}-1)\\ t_{\mathrm{pp}}&=t_{\mathrm{p}}\end{aligned}\right\}\ 0\le t_{\mathrm{p}}\le\tau_{\mathrm{p}}\tag{17}$$

As in the case of a single potential pulse, for any *p*-th pulse the concentration of the redox species at the electrode surface hold that:

$$b\sqrt{D_{\mathrm{O}}}\mathrm{c}_{\mathrm{O}}^{\mathrm{s(p)}}+a\sqrt{D_{\mathrm{R}}}\mathrm{c}_{\mathrm{R}}^{\mathrm{s(p)}}=b\sqrt{D_{\mathrm{O}}}\mathrm{c}_{\mathrm{O}}^{*}+a\sqrt{D_{\mathrm{R}}}\mathrm{c}_{\mathrm{R}}^{*}\tag{18}$$

which can be also extended to the whole concentration profile only if $\gamma=1$:

$$b\mathrm{c}_{\mathrm{O}}^{(\mathrm{p})}(x,t)+a\mathrm{c}_{\mathrm{R}}^{(\mathrm{p})}(x,t)=b\mathrm{c}_{\mathrm{O}}^{*}+a\mathrm{c}_{\mathrm{R}}^{*}\qquad(\forall\ x,\ t)\tag{19}$$

For the case of cyclic staircase voltammetry (CSV) where all the potential pulses have the same duration (τ), the following expression is obtained for the dimensionless current-potential response:

$$\Psi^{(p)}=\frac{I^{(p)}}{FA\left(c_O^*+c_R^*\right)\sqrt{\frac{D_O F v}{RT}}}=\frac{n}{a}\frac{1}{\sqrt{\pi\frac{F\Delta E}{RT}}}\sum_{m=1}^{p}\frac{F\left(\eta_{m-1}\right)-F\left(\eta_m\right)}{\sqrt{p-m+1}} \tag{20}$$

where $v=\Delta E/\tau$ is the scan rate, ΔE the step potential and:

$$F\left(\eta_m\right)=\frac{c_O^{s(m)}}{c_O^*+c_R^*} \tag{21}$$

Following the procedure indicated in the Supporting Information, the surface concentrations of the redox species are determined by solving the bvp given by Eqs. (SI.12)-(SI.15) at the *p-th* potential pulse applied. Then, the concentrations profiles and the current-potential response are obtained by substituting the expression (or value) of $c_O^{s(m)}$ in Eqs. (16) and (20). Note that, as proven elsewhere [19], the response in cyclic voltammetry can be modelled with Eq. (20) by using a sufficiently small value of the step potential (ΔE < 0.01 mV [16,18,19]).

The 2:1, 3:1, 1:2 and 1:3 stoichiometries

For the 2:1, 1:2, 3:1 and 1:3 stoichiometries, explicit solutions can be found for the surface concentrations and voltammetric response (see Supporting Information) so that:

$$\begin{aligned}
F\left(\eta_m\right)&=\left(c_O^*+\frac{2}{\gamma}c_R^*\right)\frac{\sqrt{e^{2\eta_m}+8e^{\eta_m}}-e^{\eta_m}}{4\left(c_O^*+c_R^*\right)} \quad \left(\text{2:1 stoichiometry}\right)\\
F\left(\eta_m\right)&=\frac{2\gamma c_O^*+c_R^*}{2\gamma\left(c_O^*+c_R^*\right)}+\left(c_O^*+\frac{c_R^*}{2\gamma}\right)\left(\frac{1-\sqrt{1+8e^{\eta_m}}}{4e^{\eta_m}\left(c_O^*+c_R^*\right)}\right) \quad \left(\text{1:2 stoichiometry}\right)
\end{aligned} \tag{22}$$

$$\begin{aligned}
F\left(\eta_m\right)&=-\frac{\left(c_O^*+\frac{3}{\gamma}c_R^*\right)}{\left(c_O^*+c_R^*\right)}\sqrt{\frac{e^{\eta}}{3}}\sinh\left(\frac{1}{3}\operatorname{asinh}\left(-3\sqrt{\frac{3}{e^{\eta}}}\right)\right) \quad \left(\text{3:1 stoichiometry}\right)\\
F\left(\eta_m\right)&=\frac{\left(c_O^*+\frac{1}{3\gamma}c_R^*\right)}{\left(c_O^*+c_R^*\right)}\left[1+\sqrt{\frac{1}{3e^{\eta}}}\sinh\left(\frac{1}{3}\operatorname{asinh}\left(-3\sqrt{3e^{\eta}}\right)\right)\right] \quad \left(\text{1:3 stoichiometry}\right)
\end{aligned} \tag{23}$$

with:

$$\begin{aligned}
\eta_0&=\frac{nF}{RT}\left(E_{eq}-E_{1/2}\right) \quad \text{for } m=0\\
\eta_m&=\frac{nF}{RT}\left(E_m-E_{1/2}\right) \quad \text{for } m>0
\end{aligned} \tag{24}$$

where the equilibrium potential (E_{eq}) is given by:

$$E_{eq} = E^{0'} + \frac{RT}{nF} \ln \left[\frac{\left(c_O^* \right)^a}{\left(c_R^* \right)^b} \right] \tag{25}$$

so that $F(\eta_0) = \frac{c_O^*}{c_O^* + c_R^*}$; note that concentrations are referred to the molar scale. The expressions for the surface concentrations in each pulse and so for functions $F(\eta_m)$ are formally the same for all the applied pulses (including m = 1) only differing in the value of η_m .

RESULTS AND DISCUSSION

Diagnostic criteria based on the CV shape

Attending to the experimental systems indicated in the Introduction, the key diagnostic features of the cyclic voltammograms of the 2:1, 1:2, 3:1 and 1:3 E mechanisms with n=2 are studied in Figure 1 for the most frequent situation where only one redox species is initially present. The relative and absolute positions of the peaks differ from those of the 1:1 E mechanism as reflected on the values of the potentials of the forward ($E_{p,f}$) and backward ($E_{p,b}$) peaks and on the peak-to-peak separation ($\Delta E_{pp} = \left|E_{p,f} - E_{p,b}\right|$) (see Table 1). Note that the ΔE_{pp}-value enables us to discriminate between the unity and the 2:1 and 1:2 stoichiommetries (ΔE_{pp} being in both cases between the values of the 1:1 stoichiometry with n=1 and n=2), though not between the unity and the 3:1 and 1:3 stoichiommetries that show a peak-to-peak separation similar to that of the E mechanism with n=1.

With regard to the peak currents, the magnitude of the forward peak ($I_{p,f}$, or $\Psi_{p,f}$ in dimensionless form) of complex stoichiommetries is comparable to that of the 1:1 case with the same number of electrons transferred *per* molecule (*n*/*a*) (see Figure 1), though the deviations with respect to the predictions of the well-known Randles-Sevcik equation[16,20–23] are quantitatively significant and experimentally detectable (> 10%, see Table 1). The ratio between the peak currents in the forward and backward scans ($\Psi_{p,f} / \Psi_{p,b}$, see Chapter 6 in [22]) is another parameter of interest that is proposed to unveil coupled chemical reactions when its value differs from the unity that corresponds to reversible 1:1 E mechanism[22]. As shown in Figure 1, when complex stoichiometries are considered, $\Psi_{p,f} / \Psi_{p,b}$ is close to 1 in the 2:1 case, slightly larger in the 3:1 stoichiometry and significantly smaller (<0.9) in the 1:2 and 1:3 cases.

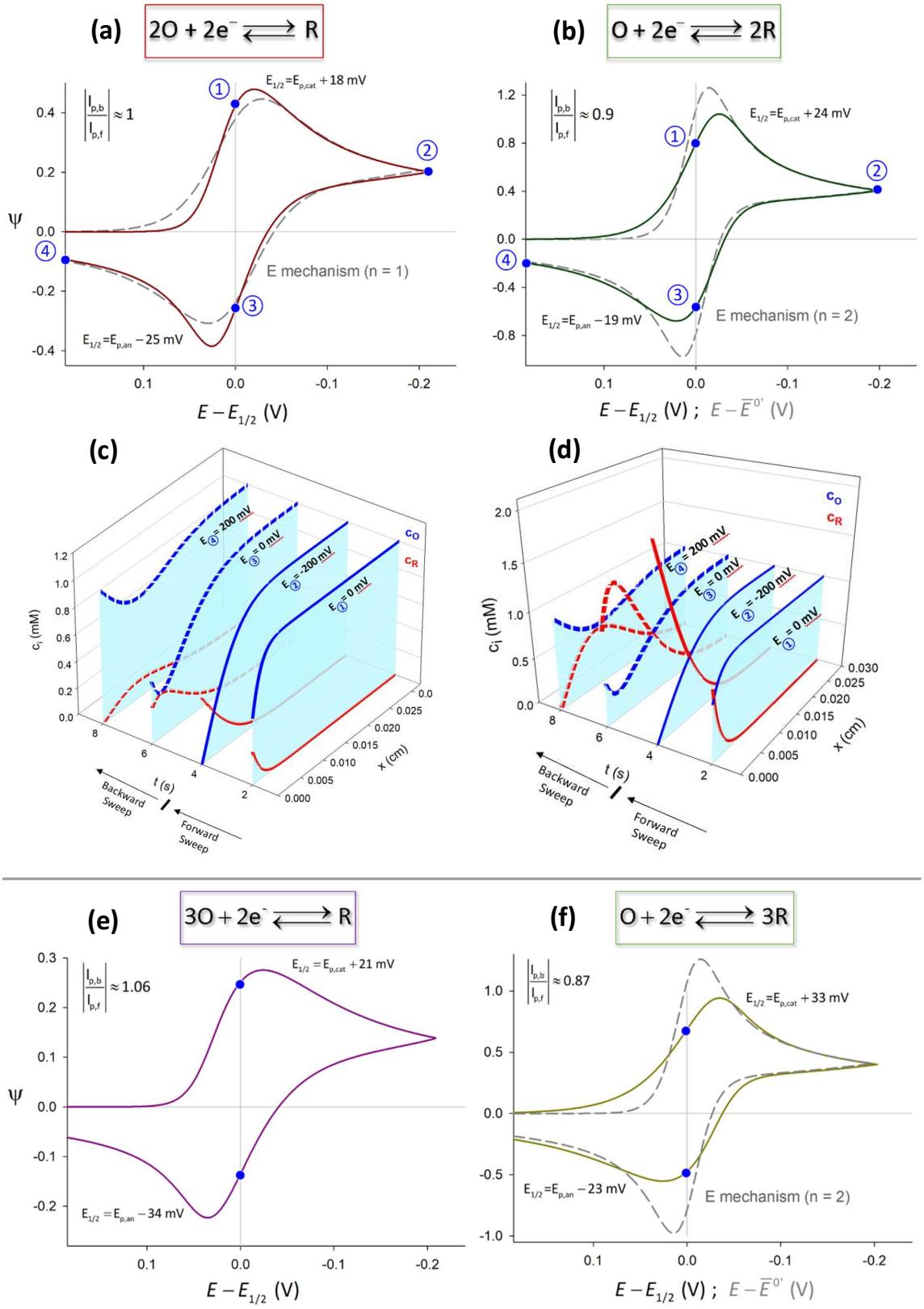

Figure 1. Cyclic voltammograms (Eq. (20)) of the 2:1 **(a)**, 1:2 **(b)**, 3:1 **(e)** and 1:3 **(f)** mechanisms for n=2. The concentration profiles (Eqs. (16)) of the redox species in the 2:1 **(c)** and 1:2 **(d)** mechanisms are also plotted at two points of the forward and reverse scans (indicated on the graphs). $\Delta E = 0.01$ mV, $c_R^* = 0$, T = 298.15 K.

Mechanism	$I_{f,p}$	$\Psi_{f,p} = \frac{I_{f,p}}{FAc_O^* \sqrt{\frac{D_O F v}{RT}}}$	$\Delta E_{pp}\,(mV)$ **	Decrease of c_O^*
3:1	$\propto v^{1/2}$	0.1011 $n^{3/2}$	109/n	Shift to negative potentials
2:1		0.1766 $n^{3/2}$	84/n	Shift to negative potentials
1:1		0.4463 $n^{3/2}$	57/n	Unaffected
1:2		0.3843 $n^{3/2}$	84/n	Shift to positive potentials
1:3		0.3460 $n^{3/2}$	109/n	Shift to positive potentials

Table 1. Summary of criteria for the elucidation of the 2:1, 1:2, 3:1 and 1:3 E mechanisms based on the features of the cyclic voltammetry response. c_R^* = 0. ** T = 298.15 K, $E_{vertex} \to -\infty$.

The concentration profiles of the redox species for the 2:1 and 1:2 stoichiometries are also shown in Figures 1c and 1d at different moments of the scan. In general, the profiles of the reduced and oxidized species are asymmetric unlike in the 1:1 case under the same conditions ($c_R^* = 0$ and $\gamma = 1$). In the forward scan towards negative potentials, the concentration of species O is steadily depleted near the electrode as it is reduced to R. As expected, the accumulation of species R in the vicinity of the electrode surface is remarkably larger in the 1:2 mechanism than in the 2:1 case. In the reverse scan, species R is oxidized back to species O once positive enough potential values are reached. In this potential region, the profiles of species R and O show a maximum or a minimum, respectively, as a consequence of the amount of species previously generated or consumed in the experiment, which is not fully balanced by diffusion.

Effect of the scan rate

The effect of the scan rate (v) on the cyclic voltammograms is considered in Figure 2, finding that the influence is totally analogous to that described for the reversible 1:1 E mechanism [16,22,23]. Thus, the peak current scales linearly with the square root of v, while the shape and position (*i.e.*, the peak potentials) of the voltammogram are independent of v. Moreover, for any stoichiometric coefficients,

an isopoint corresponding to null current is observed [19] so that the current in the reverse scan turns from positive to negative at the same potential whatever the scan rate employed.

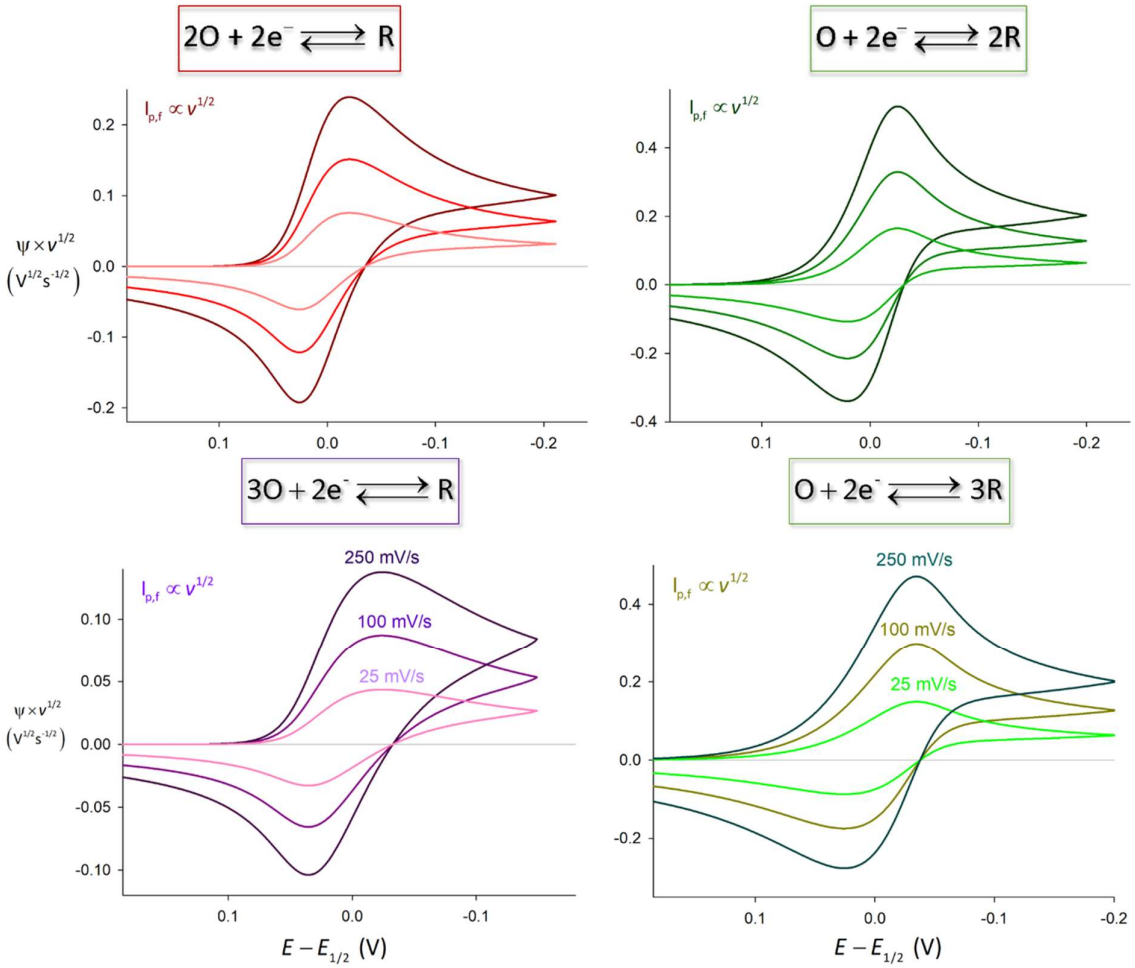

Figure 2. Influence of the scan rate (v = 25, 100 and 250 mV/s) on the CV response (Eq. (20)) of different non-unity mechanisms with n = 2. Other conditions as in Figure 1.

Effect of the reactant concentration

As can be concluded from Eq. (5), when the values of the stoichiometric coefficients *a* and *b* differ, the half-wave potential depends on the bulk concentrations of the redox species (c_O^* and c_R^*). Hence, a distinctive behaviour of the voltammetry of nonunity stoichiommetries is that the position of the signal depends on the initial concentration of the redox species.

The influence of the reactant concentration (species O in our case) is studied in Figure 3, being more significant in the 3:1 and 1:3 cases as expected attending to the c_O^*–dependence predicted by the expression for the half-wave potential (Eq. (5)). Thus, the CV signals shifts *ca*. 29mV *per* decade of

reactant concentration (c_O^*) in the 2:1 and 1:2 stoichiometries and *ca*. 58mV *per* decade in the 3:1 and 1:3 cases. The shift takes place towards more positive potentials as the bulk concentration of species O is increased for $a > b$, while the opposite behaviour is observed for $a < b$. This contrasts with the 1:1 case where c_O^* only has a scaling effect on the voltammograms without affecting the position. Hence, the stoichiometry of the electrode reaction can be revealed experimentally from the shift of the signal when modifying the bulk concentration of the reactant species.

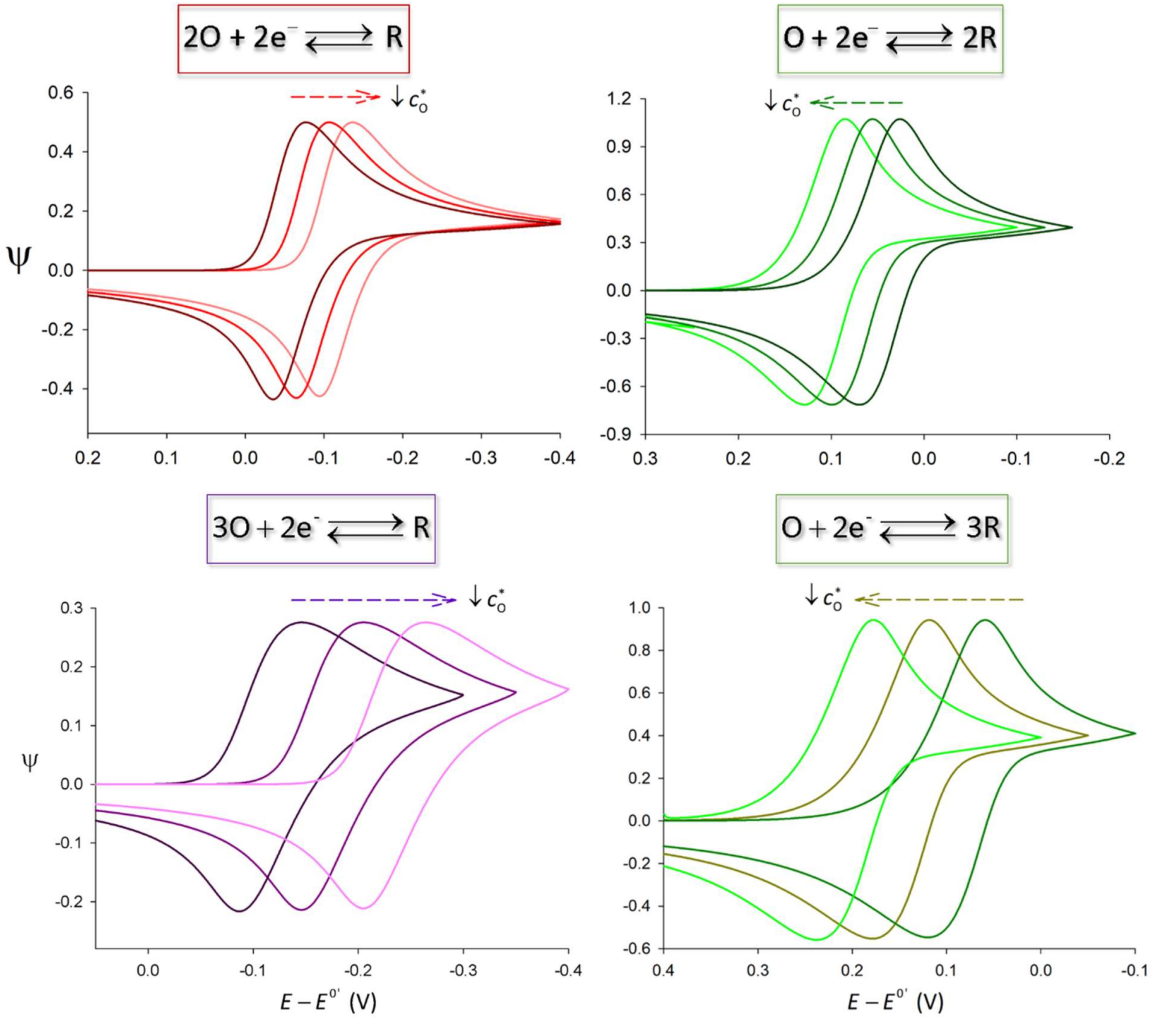

Figure 3. Influence of the bulk concentration of species O (c_O^* = 10^{-4}, 10^{-3} and 10^{-2} M) on the CV response (Eq. (20)) of different non-unity mechanisms with n = 2. Other conditions as in Figure 1.

CONCLUSIONS

A rigorous yet simple analytical theory has been developed to model the voltammetry of reversible electrode reactions with nonunity stoichiometry (*a*:*b*) at macroelectrodes. The general mathematical form of the concentration profiles and of the relationship between the surface concentrations of the redox species have been demonstrated to be the same for any stoichiometric and diffusion coefficients and in any voltammetric technique. Also, the surface concentrations are deduced to be time-independent so that the superposition principle is applicable for any *a*:*b* values and, hence, a general solution for multipulse techniques could be deduced.

For the 2:1, 1:2, 3:1 and 1:3 stoichiometries, explicit solutions have been obtained for the current-potential response, surface concentrations and concentrations profiles in cyclic voltammetry (CV). The CV curves show distinctive features and behaviours for nonunity stoichiometry, specifically, the values of the forward peak current ($I_{p,f}$) and the peak-to-peak separation (ΔE_{pp}) deviate significantly from the values expected for the 1:1 stoichiometry with the same number of electrons transferred *per* molecule, and the position of the signal depends on the concentration of the reactant species (c_O^*). Accordingly, once the *n/a*-value has been determined, for example, via diffusion-controlled chronoamperometry, the stoichiometry can be revealed from the ΔE_{pp} and $I_{p,f}$ values and the shift of the peak positions with c_O^*, for which simple analytical expressions have been given here. On the other hand, the scan rate (*v*) have the same influence on the CV curves whatever the stoichiometric coefficients so that the forward peak current scales with $v^{1/2}$ and there is an isopoint corresponding to null current.

Acknowledgements

The authors greatly appreciate the financial support provided by the Fundacion Séneca de la Región de Murcia (Project 19887/GERM/15).

ASSOCIATED CONTENT

Supporting Information

Analytical resolution of the boundary value problem of the *a:b* E mechanism at macroelectrodes in a first potential pulse (Section SI-1), double potential pulse (Section SI-2) and multipulse tecniques (Section SI-3). Study of the effect of the diffusion coefficient and bulk concentration of the product of the electrode reaction on the cyclic voltammetry (Section SI-4).

References

(1) Ito, H.; Hasegawa, Y.; Ito, Y. Electrode Behavior of Hydride Ion in Molten Alkali Chlorides. *J. Electrochem. Soc.* **2002**, *149* (8), E273. https://doi.org/10.1149/1.1485775.

(2) Dryhurst, G.; Elving, P. J. Electrooxidation of Halides at Pyrolytic Graphite Electrode in Aqueous and Acetonitrile Solutions. *Anal. Chem.* **1967**, *39* (6), 606–615. https://doi.org/10.1021/ac60250a014.

(3) Klymenko, O. V.; Compton, R. G. Mass Transport Corrected Tafel Analysis for Electrochemically Reversible Systems of Complex Stoichiometry. *J. Electroanal. Chem.* **2004**, *571* (2), 207–210. https://doi.org/10.1016/j.jelechem.2004.05.011.

(4) Bentley, C. L.; Bond, A. M.; Hollenkamp, A. F.; Mahon, P. J.; Zhang, J. Electrode Reaction and Mass-Transport Mechanisms Associated with the Iodide/Triiodide Couple in the Ionic Liquid 1-Ethyl-3-Methylimidazolium Bis(Trifluoromethanesulfonyl)Imide. *J. Phys. Chem. C* **2014**, *118* (39), 22439–22449. https://doi.org/10.1021/jp506990e.

(5) Bennett, B.; Chang, J.; Bard, A. J. Mechanism of the Br^-/Br_2 Redox Reaction on Platinum and Glassy Carbon Electrodes in Nitrobenzene by Cyclic Voltammetry. *Electrochim. Acta* **2016**, *219*, 1–9. https://doi.org/10.1016/j.electacta.2016.09.129.

(6) Kolthoff, I. M.; Miller, C. S. Anodic Waves Involving Electroöxidation of Mercury at the Dropping Mercury Electrode. *J. Am. Chem. Soc.* **1941**, *63* (5), 1405–1411. https://doi.org/10.1021/ja01850a077.

(7) Heyrovsky, J.; Kuta, J. *Principles of Polarography*; Elsevier, 1965. https://doi.org/10.1016/C2013-0-10851-3.

(8) Shuman, M. S. Nonunity Electrode Reaction Orders and Stationary Electrode Polarography. *Anal. Chem.* **1969**, *41* (1), 142–146. https://doi.org/10.1021/ac60270a014.

(9) Jaworski, A.; Stojek, Z.; Osteryoung, J. G. Oxidation of Mercury Microelectrodes in Complexing Media in the Presence and Absence of Supporting Electrolyte: *J. Electroanal. Chem.* **2003**, *558* (1–2), 141–153. https://doi.org/10.1016/S0022-0728(03)00389-9.

(10) Lin, C.; Jiao, X.; Tschulik, K.; Batchelor-McAuley, C.; Compton, R. G. Influence of Adsorption Kinetics upon the Electrochemically Reversible Hydrogen Oxidation Reaction. *J. Phys. Chem. C* **2015**, *119* (28), 16121–16130. https://doi.org/10.1021/acs.jpcc.5b04293.

(11) Jaworski, A.; Donten, M.; Stojek, Z.; Osteryoung, J. G. Conditions of Strict Voltammetric Reversibility of the H^+/H_2 Couple at Platinum Electrodes. *Anal. Chem.* **1999**, *71* (1), 243–246. https://doi.org/10.1021/ac9804240.

(12) Kätelhön, E.; Batchelor-McAuley, C.; Compton, R. G. Voltammetric Peak Heights of the Proton–Hydrogen Redox Couple: A Comprehensive Analysis. *J. Phys. Chem. C* **2015**, *119* (40), 23203–

23210. https://doi.org/10.1021/acs.jpcc.5b06040.

(13) Costentin, C.; Di Giovanni, C.; Giraud, M.; Savéant, J.-M.; Tard, C. Nanodiffusion in Electrocatalytic Films. *Nat. Mater.* **2017**, *16* (10), 1016–1021. https://doi.org/10.1038/nmat4968.

(14) Jiao, X.; Batchelor-McAuley, C.; Kätelhön, E.; Ellison, J.; Tschulik, K.; Compton, R. G. The Subtleties of the Reversible Hydrogen Evolution Reaction Arising from the Nonunity Stoichiometry. *J. Phys. Chem. C* **2015**, *119* (17), 9402–9410. https://doi.org/10.1021/acs.jpcc.5b01864.

(15) Galvez, J.; Albadalejo, J.; Molina, A. Polarografía DC: Curvas Corriente-Potencial de Procesos de Electrodo Con Ordenes de Reaccion Electroquimicos Diferentes a La Unidad. *An. Quim.* **1987**, *83*, 577–585.

(16) Molina, A.; Gonzalez, J. *Pulse Voltammetry in Physical Electrochemistry and Electroanalysis*; Monographs in Electrochemistry; Springer International Publishing: Cham, 2016. https://doi.org/10.1007/978-3-319-21251-7.

(17) Jaworski, A.; Osteryoung, J. G. General Time-Dependent Mass Balance Equation. *J. Electroanal. Chem.* **2001**, *498* (1–2), 44–50. https://doi.org/10.1016/S0022-0728(00)00219-9.

(18) Molina, A.; Serna, C.; Camacho, L. Conditions of Applicability of the Superposition Principle in Potential Multipulse Techniques: Implications in the Study of Microelectrodes. *J. Electroanal. Chem.* **1995**, *394* (1–2), 1–6. https://doi.org/10.1016/0022-0728(95)04005-9.

(19) Moreno, M. M.; Molina, A. Further Applications of Cyclic Voltammetry with Spherical Electrodes. *Collect. Czechoslov. Chem. Commun.* **2005**, *70* (2), 133–153. https://doi.org/10.1135/cccc20050133.

(20) Randles, J. E. B. A Cathode Ray Polarograph. Part II.—The Current-Voltage Curves. *Trans. Faraday Soc.* **1948**, *44*, 327–338. https://doi.org/10.1039/TF9484400327.

(21) Ševčík, A. Oscillographic Polarography with Periodical Triangular Voltage. *Collect. Czechoslov. Chem. Commun.* **1948**, *13*, 349–377. https://doi.org/10.1135/cccc19480349.

(22) Bard, A. J.; Faulkner, L. R. *Electrochemical Methods. Fundamentals and Applications*; John Wiley & Sons, Inc.: New York, 2001.

(23) Compton, R. G.; Banks, C. E. *Understanding Voltammetry*; Imperial College Press, 2010. https://doi.org/10.1142/p726.

For Table of Contents Only

$$aO + ne^- \rightleftharpoons bR$$

Mechanism	$\Psi_{f,p}$	ΔE_{pp} (mV)	Shift with c_O^* decrease?
3:1	0.1011 $n^{3/2}$	109/n	Yes, to negative
2:1	0.1766 $n^{3/2}$	84/n	Yes, to negative
1:1	0.4463 $n^{3/2}$	57/n	No
1:2	0.3843 $n^{3/2}$	84/n	Yes, to positive
1:3	0.3460 $n^{3/2}$	109/n	Yes, to positive